

## A qP-wave propagator using staggered grid in 2D VTI media

He Liu, Daniel Trad and Kristopher Innanen  
University of Calgary

### Summary

In a vertical transversely isotropic (VTI) medium, qP- and qSV- waves are intrinsically coupled as described in elastic wave equations. Therefore, when we perform elastic reverse time migration and imaging processes to qP-waves, qSV-wave energy will introduce crosstalk noise to the imaging results. In this study, instead of separating qP-waves from elastic waves, we develop a first-order wave propagator of pseudo-pure-qP-wave in 2D heterogeneous VTI media using a staggered-grid scheme. We have performed this algorithm to simulate qP-waves propagating in VTI media with weak/strong anisotropy and a two-layer VTI model, the synthetic results validate the feasibility of this algorithm.

### Method

The wavefield separation procedure (Yan and Sava, 2008) can be split into a two-steps scheme (Cheng and Kang, 2013). First, project the original qP-wavefield onto isotropic references through the introduction of a similarity transformation to the Christoffel matrix and get the transformed Christoffel matrix. Through inverse Fourier transform of the equivalent Christoffel equation of qP-wave, we obtain the second-order pseudo-pure-qP-wave equations expressed as below:

$$\begin{aligned}\rho \frac{\partial^2 u_x}{\partial t^2} &= C_{11} \frac{\partial^2 u_x}{\partial x^2} + C_{44} \frac{\partial^2 u_x}{\partial z^2} + (C_{13} + C_{44}) \frac{\partial^2 u_z}{\partial x^2} \\ \rho \frac{\partial^2 u_z}{\partial t^2} &= C_{44} \frac{\partial^2 u_z}{\partial x^2} + C_{33} \frac{\partial^2 u_z}{\partial z^2} + (C_{13} + C_{44}) \frac{\partial^2 u_x}{\partial z^2}\end{aligned}$$

Since velocity fields can be separated as well as displacement fields (Zhang and McMechan, 2010), we further derive the first-order equations to simulate separated scalar qP-waves by following procedures. Using the staggered-grid scheme (Virieux, 1986; Liu et al., 2018), we introduce velocity and stress fields as intermediate variables. In this way, we obtain the first-order pseudo-pure-qP-wave equations:

$$\begin{aligned}\frac{\partial \sigma_{xx}}{\partial t} &= C_{11} \frac{\partial v_x}{\partial x} - C_{44} \frac{\partial v_z}{\partial z} + (C_{13} + C_{44}) \frac{\partial v_z}{\partial x} \\ \frac{\partial \sigma_{zz}}{\partial t} &= C_{33} \frac{\partial v_z}{\partial z} - C_{44} \frac{\partial v_x}{\partial x} + (C_{13} + C_{44}) \frac{\partial v_x}{\partial z} \\ \frac{\partial \sigma_{xz}}{\partial t} &= C_{44} \left( \frac{\partial v_z}{\partial x} + \frac{\partial v_x}{\partial z} \right) \\ \rho \frac{\partial v_x}{\partial t} &= \frac{\partial \sigma_{xx}}{\partial x} + \frac{\partial \sigma_{xz}}{\partial z} \\ \rho \frac{\partial v_z}{\partial t} &= \frac{\partial \sigma_{xz}}{\partial x} + \frac{\partial \sigma_{zz}}{\partial z}\end{aligned}$$

In addition, applying the Thomsen notation (Thomsen, 1986), the first-order equations can be rewritten as below:

$$\begin{aligned}\frac{\partial \sigma_{xx}}{\partial t} &= \rho v_{px}^2 \frac{\partial v_x}{\partial x} - \rho v_{s0}^2 \frac{\partial v_z}{\partial z} + \sqrt{\rho^2 (\rho v_{p0}^2 - \rho v_{s0}^2) (\rho v_{pn}^2 - \rho v_{s0}^2)} \frac{\partial v_z}{\partial x} \\ \frac{\partial \sigma_{zz}}{\partial t} &= \rho v_{p0}^2 \frac{\partial v_z}{\partial z} - \rho v_{s0}^2 \frac{\partial v_x}{\partial x} + \sqrt{\rho^2 (\rho v_{p0}^2 - \rho v_{s0}^2) (\rho v_{pn}^2 - \rho v_{s0}^2)} \frac{\partial v_x}{\partial z}\end{aligned}$$

$$\begin{aligned}\frac{\partial \sigma_{xz}}{\partial t} &= \rho v_{s0}^2 \left( \frac{\partial v_z}{\partial x} + \frac{\partial v_x}{\partial z} \right) \\ \rho \frac{\partial v_x}{\partial t} &= \frac{\partial \sigma_{xx}}{\partial x} + \frac{\partial \sigma_{xz}}{\partial z} \\ \rho \frac{\partial v_z}{\partial t} &= \frac{\partial \sigma_{zx}}{\partial x} + \frac{\partial \sigma_{zz}}{\partial z}\end{aligned}$$

There will still be some residual qSV-wave energy in the wavefields simulated by the first-order qP-wave equations. Applying the same filtering algorithm (Cheng and Kang, 2013), we can obtain pure separated scalar qP-waves. On a staggered grid,  $v_x$  and  $v_z$  fields are distributed half a grid away from each other in both  $x$ - and  $z$ -axis directions. Therefore, they should be phase shifted before the filtering algorithm is performed (Liu et al., 2018).

## Results

In this work, we simulate qP-wave propagation in homogeneous VTI and layered models with size of 2 km  $\times$  2 km. For comparison, we also present the qP-waves using original elastic wave equations. In the first case, we apply the algorithm to a homogeneous VTI medium with weak anisotropy. The Thomsen parameters are as follows:  $v_{p0} = 3000$  m/s,  $v_{s0} = 1500$  m/s,  $\rho = 2500$  kg/m<sup>3</sup>,  $\epsilon = 0.1$  and  $\delta = 0.05$ . Using Rommel's (Rommel, 1994) method, we calculate the normalized  $x$ - and  $z$ -components of wavenumber domain and corresponding spatial domain deviation operators. The synthetic wavefields in VTI medium are shown in Figure 1. The  $x$ - and  $z$ -components of qSV-wavefields in Figure 1c and 1d are in different phases, the summation of both components in Figure 1e reserves qP-waves in the VTI medium while leaving some residual qSV-wave energy in the physical domain. As shown in Figure 1f is the separated scalar qP-wave, where qSV-wave energy is completely removed with the filtering algorithm.

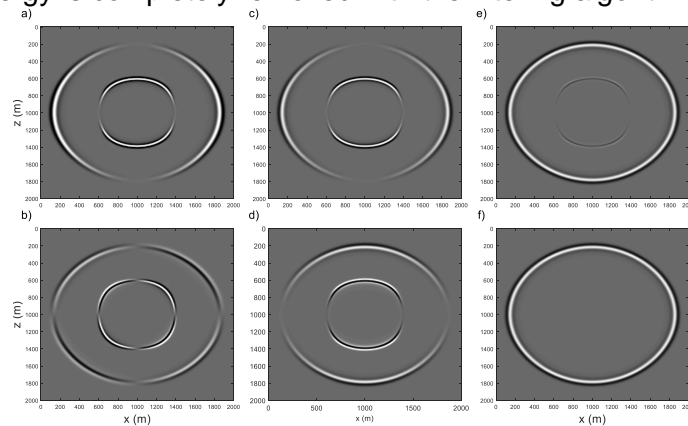


Figure 1: Synthetic wavefields in a VTI medium with weak anisotropy; a)  $x$ - and b)  $z$ -component simulated by original elastic wave equations; c)  $x$ - and d)  $z$ -component simulated by first-order pseudo-pure-qP-wave equations; e) summation of qP-wave components; f) separated scalar qP-wave.

In the second case, we apply the algorithm to a VTI medium with strong anisotropy, whose elastic parameters:  $C_{11}$  is 23.87 GPa,  $C_{33}$  is 15.33 GPa,  $C_{13}$  is 9.79 GPa,  $C_{44}$  is 2.77 GPa and density is 2500 kg/m<sup>3</sup>. The synthetic wavefields are shown in Figure 2. From the comparison between Figure 2e and 2f, we can see the qSV-wave energy can be also completely eliminated and scalar pseudo-qP-wave can be obtained after the filtering algorithm.

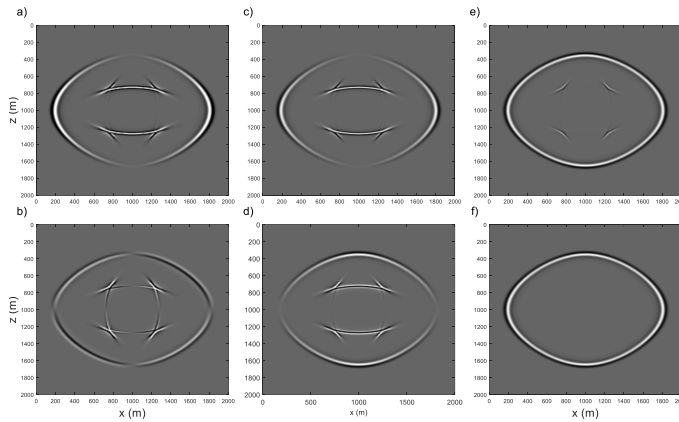


Figure 2: Synthetic wavefields in a VTI medium with strong anisotropy: a) x- and b) z-component simulated by original elastic wave equations; c) x- and d) z-component simulated by first-order pseudo-pure-qP-wave equations; e) summation of qP-wave components; f) separated scalar qP-wave.

In the last case, we simulate the qP-wavefields in a heterogeneous two-layered VTI model, in which the first and the second layer are the same VTI media with strong and weak anisotropy, respectively. The force source is also located right in the middle of the model with the interface at depth of 1.2 km. Synthetic qP-wavefields are shown in Figure 3. We can notice the converted qSV-wavefields emerge at the interface. By the summation of x- and z-components of synthetic wavefields shown in Figure 3e, some of qSV-wavefields are already seriously suppressed. In this heterogeneous model, we have to perform the filtering algorithm using the spatial domain deviation operators, after which all residual qSV-wave energy is eliminated and pure scalar qP-wave is obtained as shown in Figure 3f.

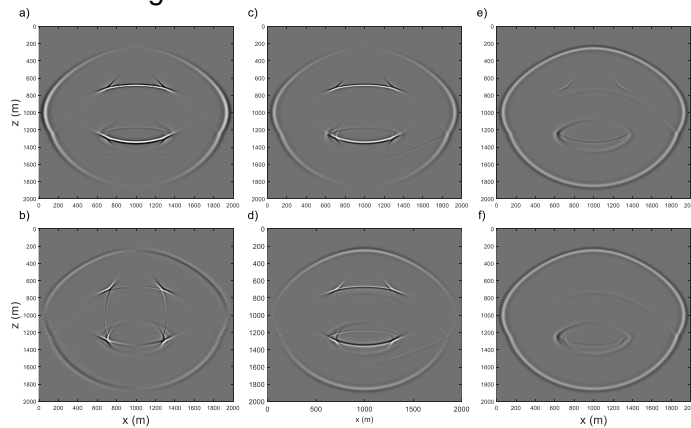


Figure 3: Synthetic wavefields in a layered VTI model: a) x- and b) z-component simulated by original elastic wave equations; c) x- and d) z-component simulated by first-order pseudo-pure-qP-wave equations; e) summation of qP-wave components; f) separated scalar qP-wave.

## Conclusions

In this study, we present a first-order qP-wave propagator in general 2D VTI media using staggered-grid scheme. Similar to our first-order qSV-wave propagator in previous study, we also need to phase shift the velocity fields before performing the filtering algorithm. We have applied the algorithm to homogeneous anisotropic VTI media with weak/strong anisotropy and a

heterogeneous layered VTI model, the synthetic results demonstrated that the algorithm is capable of simulating pure qP-wave propagation in general VTI media.

## Acknowledgements

This work was funded by the industrial sponsors of the Consortium for Research in Elastic Wave Exploration Seismology (CREWES), and by the NSERC grants CRDPJ 461179-13 and CRDPJ 543578-19. We gratefully acknowledge continued support.

## References

- Cheng, J., and Kang, W., 2013, Simulating propagation of separated wave modes in general anisotropic media, part i: qp-wave propagators: *Geophysics*, **79**, No. 1, C1–C18.
- Cheng, J., and Kang, W., 2016, Simulating propagation of separated wave modes in general anisotropic media, part ii: qs-wave propagators: *Geophysics*, **81**, No. 2, C39–C52.
- Liu, H., Wang, B., Ali, M., Tao, G., Yue, W., and Sun, H., 2018, A first-order qSV-wave propagator in 2d vti media, *in* 80th EAGE Conference and Exhibition 2018.
- Liu, H., and Innanen, K. A. H., 2019, A first-order quasi-SV-wave propagator in 2-dimensional vertical transversely isotropic (VTI) media: CREWES Research Report, 31, 41.1–41.15.
- Rommel, B. E., 1994, Approximate polarization of plane waves in a medium having weak transverse isotropy: *Geophysics*, **59**, No. 10, 1605–1612.
- Thomsen, L., 1986, Weak elastic anisotropy: *Geophysics*, **51**, No. 10, 1954–1966
- Virieux, J., 1986, P-SV wave propagation in heterogeneous media: Velocity-stress finite-difference method. *Geophysics*, 51(4): 889-901.
- Yan, J., and Sava, P., 2008a, Elastic wavefield separation for vti media, *in* SEG Technical Program Expanded Abstracts 2008, Society of Exploration Geophysicists, 2191–2195.
- Zhang, Q., and McMechan, G. A., 2010, 2d and 3d elastic wavefield vector decomposition in the wavenumber domain for vti media: *Geophysics*, **75**, No. 3, D13–D26.